RSC Pharmaceutics

ROYAL SOCIETY OF CHEMISTRY

PAPER

View Article Online
View Journal

Cite this: DOI: 10.1039/d5pm00261c

Kinetic modelling and *in vitro* release mechanism of levodopa from sporopollenin-based microcapsules in human blood plasma

Shwan Abdullah Hamad, *[a] Zhila Salam Othman, [a] Shilan Hiwa Hama Salih [a] and Trefa Mohammed Abdullah[a,b]

Levodopa (LD) remains the most effective therapy for Parkinson's disease; however, its short plasma half-life necessitates frequent dosing and contributes to fluctuating drug levels and motor complications. In this study, we systematically investigated the *in vitro* release behaviour of LD from sporopollenin exine microcapsules (SECs) in a clinically relevant biological medium, human blood plasma, and applied kinetic modelling to elucidate the governing release mechanism. LD-loaded sporopollenin microcapsules (0.5 g) were prepared by vacuum-assisted, pH-triggered precipitation and incubated in human plasma at 37 °C under moderate agitation (50 rpm). Release experiments were conducted over 12 h, with sequential sampling and medium replacement to maintain constant volume and sink conditions. LD concentrations were quantified by UV-Vis spectrophotometry using validated plasma-matched calibration curves. The release profile exhibited a reproducible biphasic pattern, characterised by a rapid initial phase within the first 30 min, followed by a prolonged and stable release phase extending to 12 h. Despite low fractional release, the system rapidly established a therapeutically relevant equilibrium LD concentration in plasma, indicative of reservoir-controlled drug availability rather than depletion-driven release. Kinetic modelling demonstrated that the Higuchi model provided the best fit to the concentration-time data (R^2 = 0.9955 ± 0.0008). In contrast, the Korsmeyer–Peppas model yielded a low release exponent (n = 0.209 ± 0.002), consistent with diffusion-dominated, Fickian transport. Peppas–Sahlin analysis further confirmed the predominance of diffusional mechanisms, with minimal contribution from matrix relaxation. These findings demonstrate that SECs function as stable, reservoir-type carriers that provide both rapid initial LD availability and sustained plasma concentrations under physiologically relevant conditions. This work, to our knowledge, represents the first detailed kinetic analysis of LD release from SECs in human blood plasma and highlights the potential of this natural biopolymer as a bio-regulated platform for improved LD delivery in Parkinson's disease.

Received 23rd September 2025,
Accepted 4th March 2026

DOI: 10.1039/d5pm00261c

rsc.li/RSCPharma

Introduction

Parkinson's disease is a progressive neurodegenerative disorder characterised by the selective loss of dopaminergic neurons in the substantia nigra, resulting in dopamine depletion and the emergence of cardinal motor and non-motor symptoms, including tremor, rigidity, bradykinesia, and cognitive impairment.[1,2] Levodopa (LD) remains the gold standard of pharmacotherapy, as it serves as a dopamine precursor that can cross the blood–brain barrier.[3] However, LD has a short plasma half-life of approximately 50 minutes,[4] necessitating frequent dosing and resulting in fluctuating plasma concentrations. These pharmacokinetic oscillations contribute to motor complications such as LD-induced dyskinesia and unpredictable "wearing-off" phenomena.[5,6] Although co-administration with carbidopa can modestly extend LD half-life to 60–90 minutes, it does not adequately prevent long-term motor complications.[7,8]

To address these limitations, controlled drug delivery systems have been extensively explored as a means to stabilise plasma LD concentrations, reduce dosing frequency, and minimise adverse effects through continuous dopaminergic stimulation.[9–11] Advanced therapeutic strategies, such as levodopa-carbidopa intestinal gel (LCIG), demonstrate the clinical

[a]Department of Pharmacy, College of Medicine, Komar University of Science and Technology, Qularaisi, Sulaimaniyah, Kurdistan Region, Iraq.
E-mail: shwan.abdulah@komar.edu.iq
[b]Department of Basic Science, College of Pharmacy, University of Sulaimani, Old Campus, Kurdistan Region, Iraq

benefits of constant drug delivery by reducing plasma fluctuations; however, their invasive nature limits widespread adoption.[4,12] Consequently, alternative non-invasive delivery approaches have attracted significant interest, including nanocarrier-assisted systems and polymeric delivery platforms.[13,14] Alongside synthetic carriers such as poly(lactic-*co*-glycolic acid) (PLGA) nanoparticles,[14] natural biomaterials have emerged as attractive alternatives due to their biocompatibility, structural robustness, and cost-effectiveness. Among these, sporopollenin exine microcapsules (SECs) represent a promising "green" platform for controlled drug delivery.[15,16]

Microencapsulation using sporopollenin, the highly cross-linked biopolymer forming the outer exine layer of plant spores, offers unique advantages for drug delivery applications.[17–20] Sporopollenin exhibits exceptional chemical stability, mechanical strength, and intrinsic biocompatibility, arising from its aliphatic-phenolic network and porous hollow architecture.[19–25] These properties have enabled the successful encapsulation and controlled release of a broad range of active agents, including pharmaceuticals, vitamins, nanoparticles, and even living cells.[26–32] Importantly, SECs have demonstrated robustness under gastrointestinal conditions[25] and controlled behaviour in complex biological fluids such as blood plasma, where slow plasma-mediated chemical modification and bulk erosion may occur over extended periods, while the exine structure largely remains intact over typical experimental windows.[22]

LD has previously been encapsulated within SECs, and its release behaviour has been investigated under simulated physiological or buffered conditions.[33] However, the release kinetics of LD from SECs in human blood plasma, a biologically complex medium containing proteins, enzymes, and binding components known to influence drug availability, have not yet been systematically characterised. This represents a critical knowledge gap, as release profiles obtained in simple buffer systems may not accurately capture the dynamic interactions governing drug behaviour under physiologically relevant conditions.

Given the relatively large size of SECs (20–35 μm),[33] intravenous administration is unrealistic. Instead, human plasma is employed in this study as a physiologically relevant medium to interrogate post-absorptive release behaviour, without implying systemic circulation of intact microcapsules. This approach provides insight into equilibrium-regulated and diffusion-controlled drug availability relevant to orally administered controlled-release LD formulations.

Accordingly, the present study investigates the *in vitro* release kinetics of LD from SECs in human blood plasma using zero-order, first-order, Higuchi, Korsmeyer–Peppas and Peppas–Sahlin kinetic models,[10,34] to elucidate the dominant release mechanism. Building on our earlier work characterising microcapsule morphology, particle size, encapsulation efficiency, and buffer-based release behaviour,[33] this study advances the translational relevance of sporopollenin-based delivery systems by directly addressing LD release dynamics under clinically meaningful plasma conditions.

Materials and methods

Materials

Lycopodium clavatum pollen powder was purchased from Fagron (UK). Levodopa (3,4-dihydroxy-L-phenylalanine) was obtained from Sigma-Aldrich (UK). Distilled water, acetone, phosphoric acid (85% v/v), hydrochloric acid (5 M), sodium hydroxide (2 M), triethylammonium acetate buffer (TEAA), and ethanol were of analytical grade and supplied from university stock.

Analytical instrumentation included a UV-Vis spectrophotometer (Cecil CE 7500, Cecil Instruments, UK), a pH meter (HANNA Instruments), a thermocouple, a vacuum pump, a Buchner filtration unit, and a temperature-controlled water bath.

Preparation of levodopa-loaded sporopollenin microcapsules. SECs were isolated from *L. clavatum* spores using the eco-friendly extraction protocol reported by Mundargi *et al.*,[18] which removes internal polysaccharide content while preserving exine integrity. Briefly, spores were defatted with acetone, treated with phosphoric acid to remove proteins and genetic material, and subjected to serial washing to eliminate residual inner material and surface contaminants. This streamlined protocol reduces acidolysis time to approximately 30 h and eliminates the alkaline lysis step, yielding intact exine capsules *via* a more sustainable process.

LD encapsulation was performed using the vacuum-assisted, pH-triggered precipitation method described by Paunov[23] and previously applied by our group.[33] LD was dissolved in 0.1 M HCl containing 0.6 mM Tween 20 to ensure complete solubilisation. Sporopollenin powder was compressed into a tablet to open trilite scars and remove trapped air, then immersed in the LD solution. Vacuum was applied for 10 minutes to evacuate residual air from the hollow microcapsules; upon vacuum release, the LD solution was drawn into the exine cavities. Following washing to remove externally adsorbed LD, 0.5 M TEAA buffer (pH ≈ 7) was added, allowing diffusion into the microcapsules and inducing pH-triggered precipitation of LD within the cavity. The resulting LD crystals exceeded the sporopollenin nanopore size, leading to physical entrapment within the microcapsules. LD-loaded microcapsules were washed thoroughly and dried before further use.

Encapsulation efficiency and microcapsule characterisation. Microcapsule morphology, particle size, structural integrity, and encapsulation efficiency were characterised previously.[33] The capsules exhibited hollow spherical morphology with diameters of 20–35 μm. For the freshly prepared batch used in this study, encapsulation efficiency was determined to be 65.4% for 0.5 g of sporopollenin. Detailed characterisation data are provided in the prior publication[33] and in the SI.

***In vitro* levodopa release in human blood plasma.** Pooled human plasma was aliquoted and stored at −80 °C until use, then thawed on ice and equilibrated to 37 °C before experiments. Based on prior optimisation,[33] a 0.3 g sporopollenin formulation exhibited smoother release but yielded lower LD concentrations (2.1×10^{-3} M), whereas the 0.5 g formulation

achieved higher LD release (2.76×10^{-3} M) and higher encapsulation efficiency. Accordingly, a fresh batch containing 0.5 g of LD-loaded SECs was selected for all release studies.

For release experiments, 0.5 g of LD-loaded microcapsules was suspended in V = 50 mL of human plasma and incubated at 37 °C under mild agitation (50 rpm). Samples were collected at predefined intervals (every 30 minutes from 0–5 h and every one h from 5–12 h). At each time point, V = 2 mL of supernatant was withdrawn and immediately replaced with fresh plasma to maintain constant volume and sink conditions. Samples were centrifuged at 5000 rpm for 10 minutes to remove particulates, and LD concentration was quantified by UV–Vis spectrophotometry at 280 nm using plasma-matched calibration curves. Samples with absorbance above 1.8 were diluted with blank plasma before measurement, and dilution factors were applied in all calculations to avoid stray-light errors at high absorbance. Blank plasma and sporopollenin-only controls were analysed in parallel. All measurements were performed in triplicate (n = 3).

Cumulative release calculation

Because sampling involved withdrawal and replacement of medium, cumulative LD release was calculated using a volume-corrected mass balance:

$$M_t = (V \cdot C_t) + \sum_{i=1}^{t-1} (v \cdot C_i)$$

where V is the total assay volume (50 mL), (v) is the volume of the sample withdrawn (2 mL), (C_t) is the concentration measured at time (t), and (C_i) is the concentration measured in all previous samples. Cumulative release percentages ($M_t/M_\infty \times 100$) were calculated using this corrected data, with errors determined by propagation of uncertainty. Results are reported primarily as concentration-time profiles, with percentage release included for reference where loading is defined.

Statistical analysis

Data are presented as mean cumulative LD concentration ± SEM. Ninety-five percentage confidence intervals (95% CI) were calculated where appropriate. A repeated-measures ANOVA was used to assess the effect of time on LD concentration over 18 time points (0–12 h) with three replicates per time point (n = 54 total observations). *Post-hoc* comparisons were conducted using Tukey's HSD test, with statistical significance set at $p < 0.05$. All analyses were performed using R (version 4.4.3).

Kinetic release models. To elucidate the release mechanism, LD release data were fitted to five kinetic models using nonlinear regression. All models were applied independently to each replicate dataset (LD-1, LD-2, LD-3), and kinetic parameters are reported as mean ± SD (n = 3). Model equations were as follows:

- Zero-order: $M_t = k_0 t + C_0$ (represents a constant release rate, independent of drug concentration).
- First-order: $\ln(1 - M_t/M_\infty) = -k_t$ (the release rate is proportional to the remaining drug).
- Higuchi: $M_t = k_H t^{1/2}$ (describes diffusion-controlled release from a porous matrix or reservoir system).
- Korsmeyer–Peppas: $\log (M_t/M_\infty) = \log k + n \log t$ (an empirical model for complex release mechanism; the release exponent n indicates mechanism: $n \approx 0.45$ (Fickian diffusion), $0.45 < n < 0.89$ (anomalous, $n \approx 0.89$) (Case II transport)).
- Peppas–Sahlin: $M_t/M_\infty = k_d t^m + k_r t^{2m}$ (used to decouple the contributions of Fickian diffusion (k_d) and matrix relaxation (k_r); the exponent m was fixed at 0.43, corresponding to spherical geometry).

For the Peppas–Sahlin model, the exponent m was fixed at 0.43, corresponding to spherical geometry. Because fractional release remained extremely low throughout the experiment ($M_t/M_\infty < 0.03$ at all-time points), all data fell within the conventional validity range of the Korsmeyer–Peppas model. Derived kinetic parameters (R^2, k, n, k_d, k_r) are reported as mean ± SD. In contrast, concentration data are reported as mean ± SEM, reflecting the distinct statistical nature of experimental measurements *versus* fitted parameters.

For visualisation in Fig. 1, fitted model parameters were used to reconstruct predicted concentration–time curves,

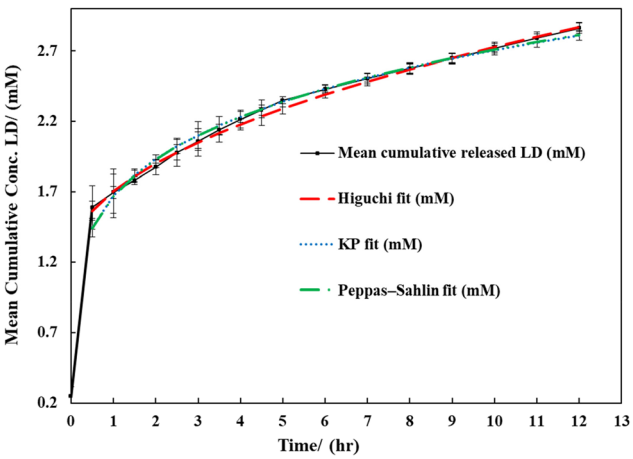

Fig. 1 Cumulative levodopa (LD) concentration–time profile from sporopollenin microcapsules (SECs) in human blood plasma at 37 °C with kinetic model overlays. Data are presented as mean cumulative LD concentration (mM) ± SEM (n = 3 independent replicates). The release profile exhibits a pronounced initial increase within the first 0.5 h (≈1.59 mM), followed by a sustained, gradual rise over 12 h, consistent with a reservoir-type release behaviour. Error bars are shown at all time points; their reduced prominence at later time points reflects low experimental variability (SEM ≈ 0.007–0.015 mM). Cumulative concentrations were corrected for sampling replacement (total volume = 50 mL; sample volume = 2 mL per time point). Experimental data are overlaid with nonlinear Higuchi, Korsmeyer–Peppas, and Peppas–Sahlin model predictions generated from replicate-wise fitted parameters and plotted directly on the original concentration–time scale. These overlays are descriptive model representations rather than linearised diagnostic plots. Corresponding linearised fits (M_t *vs.* $\sqrt{t}$ for Higuchi; log (M_t/M_∞) vs log (t) for Korsmeyer–Peppas) are provided in the SI (Fig. S4 and S5). Numerical release values and fitted parameters are summarised in Table 1 and the associated raw data files.

which were overlaid on the experimental data; these are not linearised plots.

Ethical considerations and human plasma sourcing. Human plasma samples were supplied by the Directorate of Blood Bank, Sulaimaniyah, Kurdistan Region, Iraq, as surplus material from routine diagnostic testing and were not collected specifically for this study. All samples were irreversibly anonymised before use, with no donor identifiers retained. In accordance with institutional procedures and applicable local guidelines governing the use of fully de-identified surplus biological materials, project-specific ethics committee approval and individual donor consent were not required. Plasma consisted of pooled surplus donor units collected initially in sodium heparin tubes as part of standard clinical practice.

Results and discussion

In vitro levodopa release in human blood plasma

A fresh batch of LD-loaded *Lycopodium clavatum* SECs was prepared according to the established protocol.[33] The formulation exhibited physicochemical properties and an encapsulation efficiency of 65.4%, consistent with previous reports.[33] Based on prior optimisation, the 0.5 g sporopollenin formulation was selected for release studies, as it provided higher encapsulation efficiency and improved reproducibility compared with lower-mass formulations.

LD release was evaluated in pooled human blood plasma at 37 °C to provide a physiologically relevant medium incorporating protein binding and enzymatic activity, which are absent in buffered or simulated systems. This represents a substantive advance over earlier release studies conducted in simplified media.[26,28,29,33] The cumulative LD concentration-time profile is shown in Fig. 1, with numerical values summarised in Table 1. Release behaviour is reported primarily as absolute concentration-time profiles, which directly reflect drug availability in plasma and are independent of formulation loading assumptions.

The release profile exhibits a biphasic pattern. During the initial 0.5 h, the mean cumulative LD concentration increased rapidly from 0.247 ± 0.007 mM to approximately 1.59 mM, consistent with an early burst phase. This initial increase is attributed to dissolution of surface-associated LD and diffusion through pores proximal to the exine surface. Following this phase, LD release transitioned to a markedly slower regime, with cumulative concentrations increasing gradually and reaching ~2.86 mM over 12 h. The low variability observed at later time points (SEM ≈ 0.007–0.015 mM) indicates high reproducibility across replicates.

Throughout the experiment, sink conditions were maintained by replacing each withdrawn aliquot with fresh plasma, and cumulative concentrations were calculated using a sampling-replacement correction. This approach ensures that the observed release profile reflects intrinsic carrier behaviour rather than artefacts arising from drug accumulation in the release medium.

Table 1 Mean cumulative LD concentration and derived release parameters from SECs in human blood plasma at 37 °C. Data are reported as mean cumulative LD concentration (mM) ± standard error of the mean (SEM, n = 3 independent replicates: LD-1, LD-2, LD-3). The concentration-time profile exhibits a pronounced early increase within the first 0.5 h, followed by a sustained, gradual rise over the remaining duration, consistent with reservoir-type, diffusion-regulated release behaviour. For completeness, cumulative release is additionally expressed as a percentage of the total encapsulated LD, with associated propagated error; however, release behaviour is primarily interpreted using concentration-time profiles, as fractional release values depend on formulation loading and batch history

Time (h)	Mean cumulative conc. LD (mM)	SEM ×10	Cumulative release LD (%)	% Error cumulative release ×10
0	0.2467	0.067	0.231	0.06
0.5	1.5899	0.156	1.491	0.15
1	1.6965	0.043	1.591	0.04
1.5	1.7811	0.098	1.671	0.05
2	1.844	0.064	1.738	0.06
2.5	1.977	0.096	1.853	0.09
3	2.0589	0.065	1.931	0.06
3.5	2.1403	0.039	2.008	0.04
4	2.2162	0.064	2.079	0.06
4.5	2.2819	0.056	2.141	0.05
5	2.3493	0.025	2.204	0.02
6	2.4293	0.052	2.279	0.05
7	2.5041	0.036	2.353	0.03
8	2.5714	0.036	2.418	0.03
9	2.6489	0.034	2.485	0.03
10	2.72	0.035	2.552	0.03
11	2.7909	0.033	2.618	0.03
12	2.8615	0.036	2.684	0.03

Over 5 h, the LD concentration was ~2.34 mM, compared with previous studies conducted in simulated plasma, which reported a higher apparent maximum LD concentration (~2.76 mM) at 5 h.[33] The present data demonstrate a more moderate release in human plasma. This difference is plausibly attributed to interactions between LD and plasma constituents, including proteins and enzymes known to influence drug solubility and transport. Similar plasma-mediated modulation has been reported for other sporopollenin-based systems; for example, Fan *et al.* demonstrated slow plasma-induced chemical modification of sporoderm structures without rapid loss of capsule integrity.[22]

The observed release behaviour is consistent with prior reports describing SECs as diffusion-dominated carriers for a wide range of active agents, including ibuprofen,[26] antibiotics,[27] folic acid,[28] aspirin,[29] metformin,[30] living cells,[31] and MRI contrast agents.[32] In these systems, controlled release has been attributed to the chemically robust, microporous architecture of sporopollenin.[19–25] At the molecular level, sporopollenin comprises a highly cross-linked aliphatic-phenolic network containing oxygenated functional groups that form nanoscale diffusion pathways while resisting bulk erosion. For LD, a small hydrophilic molecule containing catechol groups, hydrogen bonding with hydroxyl and carboxyl functionalities within the sporopollenin matrix is likely to retard diffusion following the initial burst phase, as reported for other encapsulated molecules.[26–30]

In contrast to conventional LD formulations, which are limited by a short plasma half-life (≈50–90 min, even with peripheral decarboxylase inhibition),[6,7] the sporopollenin system maintains a stable plasma LD concentration over the experimental time frame. Rather than a continuous, monotonic release, the data indicate rapid attainment of an equilibrium concentration, followed by minimal additional release, consistent with reservoir-controlled, equilibrium-regulated behaviour. This profile conceptually aligns with strategies aimed at stabilising plasma LD exposure, such as intestinal infusion systems,[4] while avoiding invasive administration routes.

Comparison with previously reported levodopa release systems. Most reported LD delivery systems evaluated at physiological temperature exhibit substantial cumulative release within 6–12 h. For example, poly(lactic-*co*-glycolic acid) (PLGA)-based nanoparticles and polymeric microparticles typically release approximately 30–70% of encapsulated LD over this timeframe, reflecting conventional sustained or controlled-release behaviour rather than strong drug retention.[14,35] Similarly, dialysis-based release studies conducted in buffered media at physiological pH report moderate to high LD diffusion from carrier matrices, indicating limited confinement under conditions intended to approximate systemic exposure.[36]

By contrast, fewer carrier systems have been designed to suppress premature LD release. Mesoporous silica nanoparticles, for example, exhibit minimal LD release under acidic gastric conditions; however, such systems have not been evaluated in plasma or under physiologically neutral conditions relevant to blood circulation.[37] Importantly, systematic *in vitro* studies of LD release conducted directly in human blood plasma at 37 °C remain scarce, despite plasma being a highly biorelevant medium containing proteins, lipoproteins, and enzymes known to influence nanocarrier stability and drug retention.[38]

Within this context, the present sporopollenin-based system exhibits a low fractional release of levodopa (LD) (~2–3%) after 12 h in human plasma. This behaviour reflects strong drug retention and limited premature leakage, supporting the classification of sporopollenin microcapsules (SECs) as high-retention, reservoir-type carriers rather than conventional sustained-release matrices. Accordingly, the primary objective of the present formulation is not rapid LD liberation in plasma, but rather preservation of the encapsulated drug during circulation while maintaining a therapeutically relevant equilibrium concentration in the surrounding medium. Fractional release values are therefore reported for reference, whereas mechanistic interpretation focuses primarily on the concentration–time profiles, which more directly represent LD availability in plasma.

The low fractional release (≈2–3% over 12 h) should not be interpreted as poor drug availability. Instead, it is consistent with equilibrium-regulated, reservoir-type behaviour. As the surrounding plasma approaches a characteristic equilibrium LD concentration, the net diffusion driving force decreases, resulting in an apparent release plateau. At the same time, the majority of the payload remains within the capsules. This response aligns with the highly cross-linked, non-swellable nature of sporopollenin, which exhibits strong resistance to bulk erosion over the present 12 h experimental window while favouring slow, predominantly Fickian diffusion through intrinsic nanoporous pathways. Over longer exposure times, gradual plasma-mediated chemical modification of the exine has been reported (Fan *et al.*[22]). In addition, plasma protein binding of LD is expected to lower its effective diffusivity relative to simple buffered media, further contributing to the reduced apparent fractional release.

Statistical analysis

Statistical analysis was performed on mean cumulative LD concentration-time data obtained from three independent replicates (n = 3). Because the same formulation was repeatedly sampled over time, repeated-measures analysis of variance (RM-ANOVA) was used to evaluate the effect of time (0–12 h) on LD concentration in human plasma at 37 °C.

The RM-ANOVA revealed a highly significant overall effect of time (SS = 18.9929, F = 10 563.6, $p < 1 \times 10^{-15}$), with minimal residual variance (MS = 1.06×10^{-4}), confirming that the observed changes in LD concentration were systematic rather than attributable to experimental noise (Table 2). Ninety-five percentage confidence intervals calculated at each time point (Table 3) further demonstrated excellent inter-replicate agreement, particularly during the post-burst phase (Table 4).

Post-hoc analysis using Tukey's HSD test identified statistically significant increases in LD concentration during the initial release phase (0 *vs.* 0.5 h and 0 *vs.* 1 h; $p < 0.001$). In contrast, comparisons between adjacent late time points (10 *vs.* 11 h and 11 *vs.* 12 h) were not statistically significant (p = 0.99), confirming the establishment of a concentration plateau. Although numerous pairwise comparisons are possible across the 18 time points, representative contrasts are reported to illustrate the distinct release phases without redundancy. Collectively, these results statistically support a biphasic release profile characterised by rapid initial drug availability followed by prolonged concentration stability.

Application of kinetic models to levodopa release from sporopollenin microcapsules

Kinetic modelling was performed using release data obtained from the 0.5 g sporopollenin formulation, previously identified

Table 2 Results of repeated-measures ANOVA evaluating the effect of time on mean cumulative LD concentration released from SECs in human plasma over 12 h (n = 3). The analysis demonstrates a highly significant time effect with minimal residual variance, confirming a reproducible, time-dependent release profile

Source of variation	Sum of squares (SS)	df	Mean square (MS)	F statistic	p value
Time (cumulative)	18.9929	17	1.1172	10 563.6	$<1 \times 10^{-15}$
Residual (error)	0.00381	36	1.06×10^{-4}	—	—

Table 3 95% Confidence intervals for mean cumulative LD concentration. Mean cumulative LD concentration (mM) ± 95% confidence intervals at each sampling time point (n = 3). Narrow confidence intervals across the time course indicate high analytical precision and low inter-replicate variability, particularly during the sustained-release phase

Time (h)	Mean cumulative released conc. (mM)	95% CI (±mM)
0	0.2467	±0.0288
0.5	1.5899	±0.0671
1	1.6965	±0.0185
1.5	1.7811	±0.0120
2	1.874	±0.0232
2.5	1.9777	±0.0413
3	2.0589	±0.0280
3.5	2.1403	±0.0168
4	2.2162	±0.0275
4.5	2.2819	±0.0155
5	2.3493	±0.0108
6	2.4293	±0.0138
7	2.5047	±0.0155
8	2.5774	±0.0155
9	2.6489	±0.0146
10	2.72	±0.0151
11	2.7909	±0.0142
12	2.8615	±0.0155

as optimal based on encapsulation efficiency and release behaviour.[33] Mean cumulative LD concentration-time profiles measured in human blood plasma were analysed using zero-order, first-order, Higuchi, Korsmeyer–Peppas, and Peppas–Sahlin models. To ensure statistical robustness and to avoid artefacts associated with fitting averaged curves, all models were fitted independently to each replicate dataset (LD-1, LD-2, LD-3) using nonlinear regression, and kinetic parameters are reported as mean ± SD (n = 3) (Table 5).

Among the evaluated models, the Higuchi equation provided the best fit to the experimental concentration-time data (R^2 = 0.9955 ± 0.0008), outperforming both the zero-order and first-order models. This finding indicates diffusion-controlled transport from an internal drug reservoir rather than concentration-independent release (zero-order) or dissolution-controlled kinetics (first-order).

The Korsmeyer–Peppas model was applied strictly within its conventional validity window (≤60% fractional release). Because fractional release remained extremely low throughout the experiment (M_t/M_∞ < 0.03 at all-time points), the entire dataset lies well within the accepted fitting range for this model. The fitted release exponent was n = 0.209 ± 0.002, a value substantially below the threshold associated with anomalous transport in spherical systems ($n \approx$ 0.45–0.89). Such a low exponent is consistent with Fickian diffusion from a rigid, non-swellable reservoir-type matrix, rather than polymer relaxation-controlled or erosion-driven release.

To further resolve the relative contributions of diffusion and matrix relaxation, the Peppas–Sahlin model was employed. The fitted diffusional rate constant (k_d = 0.01551 ± 0.00008) exceeded the relaxational rate constant (k_r = (1.24 ± 0.14) × 10^{-4}) by more than two orders of magnitude, confirming that diffusion dominates LD transport in plasma. Deconvolution of the model terms showed that the Fickian contribution accounted for approximately 98.67–99.31% of total release over 0.5–12 h, while relaxational processes contributed only 0.69–1.33% (Table 6). The slight increase in relaxational contribution with time is consistent with slow plasma-mediated chemical modification of the sporopollenin exine rather than pronounced swelling or structural degradation, in agreement with sporopollenin's highly cross-linked and chemically robust architecture.[18,20,21]

Importantly, sporopollenin should not be regarded as strictly non-eroding under physiological conditions. Human blood plasma has been reported to catalyse slow bulk chemical modification of Lycopodium sporoderm microcapsules (Fan *et al.*[22]). The very small relaxational contribution (k_r) observed over the present 12 h window is therefore consistent with the early stages of this plasma-mediated modification rather than complete matrix inertness.

The correspondence between the experimental concentration–time data and the overlayed nonlinear Higuchi, Korsmeyer–Peppas, and Peppas–Sahlin models in Fig. 1 is consistent with diffusion-dominated, reservoir-controlled release behaviour. It is important to note that the overlays shown in Fig. 1 represent back-calculated nonlinear predictions generated from replicate-wise fitted parameters and are not linearised diagnostic fits. Linearised representations used for formal model assessment (M_t *vs.* $\sqrt{t}$ for Higuchi; log (M_t/M_∞) *vs.* log (t) for Korsmeyer–Peppas) are provided in the SI (Fig. S4 and S5).

Table 4 Tukey's HSD *post-hoc* analysis of mean cumulative LD concentration. Representative results of Tukey's HSD *post-hoc* test comparing mean cumulative LD concentrations between selected time points. A "reject" outcome indicates a statistically significant difference (α = 0.05). Only key contrasts are reported to highlight the initial burst, transitional, and plateau phases of release, avoiding redundancy among the 153 possible pairwise comparisons

First time point (h)	Second time point (h)	Mean difference (mM)	Adjusted p-value	95% CI Lower	95% CI Upper	Reject
0	0.5	1.3432	<0.001	1.312	1.374	Yes
0	1	1.4498	<0.001	1.419	1.481	Yes
0	12	2.6148	<0.001	2.581	2.649	Yes
0.5	1	0.1066	<0.01	0.072	0.141	Yes
1	1.5	0.0846	<0.05	0.041	0.128	Yes
10	11	0.0709	0.99	−0.028	0.17	No
11	12	0.0706	0.99	−0.029	0.17	No

Table 5 Comparison of kinetic models for LD release from SECs in human plasma. Kinetic model fitting of cumulative LD concentration-time data obtained in human blood plasma at 37 °C for the 0.5 g sporopollenin formulation. Zero-order, first-order, Higuchi, Korsmeyer–Peppas, and Peppas–Sahlin models were fitted independently to each replicate dataset (LD-1, LD-2, LD-3), and parameters are reported as mean ± SD (n = 3). The Korsmeyer–Peppas model was fitted within its conventional validity window (≤60% fractional release); notably, because M_t/M_∞ remained < 0.03 at all time points, the entire dataset falls within this range. The fitted Korsmeyer–Peppas exponent (n = 0.209 ± 0.002) indicates Fickian diffusion-controlled transport from a rigid reservoir-type system, rather than anomalous (non–Fickian) transport typical of swellable polymer matrices. Peppas–Sahlin parameters (k_d and k_r) further support a diffusion-dominant release mechanism

Kinetic model	Equation	R^2 value (mean ± SD)	Rate constant (mean ± SD)	n value (mean ± SD)	Mechanism
Zero-order	$M_t = k_0 t + C_0$	0.9517 ± 0.0003	$(9.97 \pm 0.00) \times 10^{-4}$	—	Concentration-independent (poor model fit; burst effect present)
First-order	$\ln(1 - M_t/M_\infty) = -k_t$	0.9524 ± 0.0002	$(1.009 \pm 0.000) \times 10^{-3}$	—	Concentration-dependent (poor model fit; burst effect present)
Higuchi	$M_t = k_H t^{1/2}$	0.9956 ± 0.0008	$(4.42 \pm 0.028) \times 10^{-3}$	—	Diffusion-controlled (best fit)
Korsmeyer–Peppas (nonlinear)	$\log(M_t/M_\infty) = \log k + n \log t$	0.9864 ± 0.0038	0.01563 ± 0.00009	0.2091 ± 0.0002	Diffusion dominated (low n consistent with Fickian behaviour under low fractional release)
Peppas–Sahlin	$M_t/M_\infty = k_d t^m + k_r t^{2m}$	0.9863 ± 0.0057	k_d = 0.01551 ± 0.00008; k_r = $(1.24 \pm 0.14) \times 10^{-4}$	m = 0.2091 ± 0.0002	Diffusion term dominates; relaxation contribution minor (≈0.69–1.33%)

Table 6 Time-resolved contributions of Fickian diffusion (F, %) and relaxational/structural contributions (R, %) to LD release, calculated from the Peppas–Sahlin model fits (mean ± SD, n = 3). Across 0.5–12 h, the Fickian component remains dominant (~98.67–99.31%), while relaxation contributes only ~0.69–1.33%, consistent with diffusion through a stable, highly cross-linked sporopollenin exine with minimal matrix relaxation in plasma

Time (t) (h)	Fickian (F %)	SD (F)	Relaxational (R %)	SD (R)
0.5	99.31	0.08	0.69	0.08
1	99.21	0.09	0.79	0.09
1.5	99.14	0.10	0.86	0.10
2	99.08	0.10	0.92	0.10
3	99.00	0.11	1.00	0.11
4	98.94	0.12	1.06	0.12
6	98.85	0.13	1.15	0.13
8	98.78	0.14	1.22	0.14
10	98.72	0.14	1.28	0.14
12	98.67	0.15	1.33	0.15

Taken together with the observed release plateau and the structural characteristics of sporopollenin, these findings indicate that LD transport from SECs in human plasma is primarily governed by slow Fickian diffusion through a stable, highly cross-linked exine reservoir. This behaviour supports the potential of sporopollenin as a robust platform for controlled drug delivery.[10,19,27–29,34]

Hypothesis: proposed bio-regulated sporopollenin reservoir model for levodopa delivery. We propose that *Lycopodium clavatum* SECs function as bioregulated drug reservoirs for LD, in which drug availability is primarily governed by equilibrium-driven, diffusion-controlled mechanisms rather than by time-dependent matrix erosion or complete carrier dissolution over typical experimental windows.

Sporopollenin exines exhibit exceptional chemical robustness and barrier properties, enabling retention of encapsulated LD during oral and gastric exposure. Resistance of sporopollenin to extreme acidity has been demonstrated by the survival of encapsulated living yeast cells following exposure to 0.1 M HCl.[31] Complementary taste-masking and oral delivery studies further confirm that sporopollenin limits premature drug dissolution in saliva and maintains structural integrity during oral exposure.[19,26] Consistent with this barrier function, minimal drug release under gastric-relevant conditions (~2.68% over 12 h) has been reported, supporting the hypothesis that SECs protect LD from early degradation and delay drug release beyond the stomach.

Following gastric passage, SECs are hypothesised to retain structural integrity and to retain the majority of the LD payload within gastrointestinal environments without undergoing intact epithelial translocation. Sporopollenin-based microcapsules have been shown to survive GI-relevant conditions and exhibit controlled release behaviour in aqueous media.[20,25] While systemic entry of intact 20–35 μm capsules has not been demonstrated, delayed post-gastric LD availability may arise from intestinal-wall depots, gradual dissolution-driven absorption, or partial capsule fragmentation. Accordingly, intestinal translocation pathways and *in vivo* biodistribution remain explicit translational gaps.

Upon exposure to physiological fluids, SECs are proposed to act as long-lived reservoir systems. Human blood plasma has been shown to catalyse slow, bulk chemical modification of sporopollenin without rapid surface breakdown, with approximately 85% of capsules remaining morphologically intact after 96 h.[22] Additional studies demonstrate that sporopollenin can retain and release encapsulated payloads in blood plasma without catastrophic disintegration.[27,30,32] The conceptual role of sporopollenin as a micro-reactor or reservoir system, in which nanoscale pores mediate diffusion, has been established previously.[23]

Within this framework, LD release from SECs is hypothesised to be governed by a local concentration equilibrium, resulting in a self-regulating release profile. In our previous

work, SECs established a reproducible LD plateau concentration (~2.75 mM), with cumulative release limited to ~2.6%, and release resumed upon dilution of the surrounding medium.[33] The present plasma kinetic study further confirms that LD release follows diffusion-dominated, Fickian kinetics, consistent with reservoir-controlled transport. Independent sporopollenin studies support diffusion-controlled release behaviour across multiple drug classes.[27–30]

An initial release phase occurs within approximately 30 min, establishing a local plasma LD concentration of 1.5899 mM in 50 mL of *in vitro* medium. When scaled to an average adult blood volume (5 L), this corresponds to:

$$1.5899\ \text{mM} \times 0.05\ \text{L}/5\ \text{L} = 0.0159\ \text{mM} = 15.9\ \mu\text{M}$$

This concentration falls within the clinically relevant plasma range reported for LD therapy (~10–50 μM),[6] indicating that the initial release phase is sufficient to achieve therapeutically meaningful LD levels rapidly. As systemic LD is metabolised (plasma half-life ≈ 50–90 min) or transported across the blood–brain barrier, plasma concentration decreases. This disturbance of equilibrium is hypothesised to trigger additional LD release from the internal SEC reservoir, restoring the equilibrium concentration. Such feedback-regulated behaviour may reduce pronounced peaks and troughs associated with conventional dosing, although direct *in vivo* confirmation remains necessary.

Finally, gradual plasma-mediated bulk modification of the sporopollenin exine is hypothesised to permit eventual carrier fragmentation and clearance without permanent accumulation, consistent with plasma degradation studies.[22,32]

Collectively, this hypothesis proposes that SECs operate not as passive dissolution-controlled carriers but as bio-regulated LD reservoirs, providing an initial therapeutic release followed by sustained, equilibrium-driven drug availability. While intestinal translocation and *in vivo* biodistribution remain key translational challenges, this model offers a mechanistically grounded framework for prolonged dopaminergic stimulation.

Hypothesis-aligned delivery routes. Based on the available evidence, the following delivery routes are proposed for 0.5 g (500 mg) sporopollenin powder loaded with LD:1. Oral reservoir delivery, in which SECs provide gastric protection and delayed LD availability without requiring systemic circulation of intact capsules.[17,19,20]

2. Subcutaneous or intramuscular depot delivery, where SECs may function as long-acting tissue reservoirs, leveraging demonstrated plasma stability and equilibrium-regulated release behaviour.[22,36]

3. Intranasal delivery (future optimisation), where SECs or size-modified sporopollenin formulations could protect LD from enzymatic degradation and enhance mucosal residence time, enabling sustained systemic or nose-to-brain delivery while bypassing first-pass metabolism, consistent with established intranasal LD strategies.[39–41]

Conclusion

This study provides the first systematic characterisation of LD release from SECs in a clinically relevant biological medium, human blood plasma. Under physiological conditions (pH ≈ 7.0, 37 °C, moderate agitation), the sporopollenin system exhibited a stable and highly reproducible release profile that reflects realistic plasma interactions, including protein binding and enzymatic effects. Compared with simulated plasma systems, the moderated total release observed here is consistent with LD-plasma interactions, particularly albumin binding. It aligns with prior reports on plasma-mediated modulation of sporopollenin-based carriers.[22,33]

In vitro release studies demonstrated a distinct biphasic profile, characterised by a rapid initial phase within the first 30 minutes, followed by a prolonged and stable release phase extending for at least 12 hours. This behaviour directly addresses the short plasma half-life of LD[6,7] and the pharmacokinetic fluctuations that cause motor complications in Parkinson's disease,[5] offering a strategy to reduce dosing frequency and improve patient compliance by providing sustained dopaminergic stimulation.[8,11] Repeated-measures ANOVA and *post-hoc* analyses confirmed a highly significant time-dependent effect with minimal residual variability, validating the robustness and reproducibility of the observed release behaviour.

Kinetic modelling revealed that LD release in human plasma is predominantly diffusion-controlled. The Higuchi model provided the best fit to the concentration-time data (R^2 = 0.9955 ± 0.0008).[10] In contrast, the Korsmeyer–Peppas model yielded a low release exponent (n = 0.209 ± 0.002), unequivocally indicating Fickian diffusion from a rigid reservoir-type system. Peppas–Sahlin analysis further confirmed diffusion dominance, with Fickian transport accounting for approximately 99% of the release over the experimental time course. These findings are consistent with the highly cross-linked, chemically robust architecture of sporopollenin, which enables nanoscale diffusion while resisting bulk erosion and excessive matrix relaxation over typical experimental windows.[18–21,26]

Importantly, although only a small fraction of the encapsulated LD was released over 12 hours, the system rapidly established a therapeutically relevant plasma equilibrium concentration. When scaled to physiological blood volumes, the initial release corresponds to plasma LD concentrations within the clinically effective range reported for LD therapy,[6] supporting the concept of equilibrium-regulated, reservoir-controlled drug availability rather than depletion-driven release. This behaviour distinguishes SECs from conventional sustained-release formulations and aligns with the principle of continuous dopaminergic stimulation.[11]

Collectively, these results validate SECs as a robust, natural biopolymer platform for controlled LD delivery under physiologically relevant plasma conditions. The system compares favourably with previously reported sporopollenin-based carriers[22,26–30,33] and contemporary LD delivery strategies, including intestinal infusion and advanced controlled-release

approaches,[4,6,11] while offering a unique combination of early therapeutic availability and prolonged concentration stability.

The present work is limited to *in vitro* evaluation and does not capture the full complexity of *in vivo* pharmacokinetics, metabolism, or immune interactions. Future studies should focus on *in vivo* bioavailability, tissue distribution, and therapeutic efficacy, as well as on formulation optimisation strategies, such as surface functionalisation, to further enhance circulation stability.[38] Nonetheless, this study establishes a strong mechanistic foundation for the development of sporopollenin-based, bio-regulated reservoir systems for improved LD therapy.

Conflicts of interest

There are no conflicts to declare.

Data availability

The data supporting the findings of this study will be available on request.

Supplementary information (SI) is available. See DOI: https://doi.org/10.1039/d5pm00261c.

References

1 S. Zafar and S. S. Yaddanapudi, *Parkinson disease*, StatPearls, 2023, Available from: https://www.ncbi.nlm.nih.gov/books/NBK470193/.
2 W. Poewe, K. Seppi, C. M. Tanner, G. M. Halliday, P. Brundin, J. Volkmann, *et al.*, Parkinson's disease, *Nat. Rev. Dis. Primers*, 2017, **3**(1), 17013, DOI: 10.1038/nrdp.2017.13.
3 K. R. Gandhi and A. Saadabadi, *L-Dopa*, StatPearls, 2023. Available from: https://www.ncbi.nlm.nih.gov/books/NBK482140/.
4 D. Nyholm, P. Odin, A. Johansson, K. Chatamra, C. Locke, S. Dutta, *et al.*, Pharmacokinetics of levodopa, carbidopa, and 3-O-methyldopa following 16-hour jejunal infusion of levodopa-carbidopa intestinal gel in advanced Parkinson's disease patients, *AAPS J.*, 2013, **15**(2), 316–323, DOI: 10.1208/s12248-012-9439-1.
5 B. Thanvi, N. Lo and T. Robinson, Levodopa-induced dyskinesia in Parkinson's disease: clinical features, pathogenesis, prevention and treatment, *Postgrad. Med. J.*, 2007, **83**(980), 384–388, DOI: 10.1136/pgmj.2006.054759.
6 M. Contin and P. Martinelli, Pharmacokinetics of levodopa, *J. Neurol.*, 2010, **257**(S2), 253–261, DOI: 10.1007/s00415-010-5728-8.
7 E. Leyden and P. Tadi, *Carbidopa*, StatPearls, 2023. Available from: https://www.ncbi.nlm.nih.gov/books/NBK554552/.
8 A. Antonini, P. Odin, R. Pahwa, J. Aldred, A. Alobaidi, Y. J. Jalundhwala, P. Kukreja, *et al.*, The long-term impact of levodopa/carbidopa intestinal gel on off-time in patients with advanced Parkinson's disease: a systematic review, *Adv. Ther.*, 2021, **38**(6), 2854–2890, DOI: 10.1007/s12325-021-01747-1.
9 S. Mehrotra and K. Pathak, *Controlled release drug delivery systems: principles and design*, Elsevier eBooks, 2024, pp. 3–30. DOI: 10.1016/b978-0-323-91816-9.00014-x.
10 S. Adepu and S. Ramakrishna, Controlled drug delivery systems: current status and future directions, *Molecules*, 2021, **26**(19), 5905, DOI: 10.3390/molecules26195905.
11 D. J. Van Wamelen, S. Grigoriou, K. R. Chaudhuri and P. Odin, Continuous drug delivery aiming continuous dopaminergic stimulation in Parkinson's disease, *J. Parkinson's Dis.*, 2018, **8**(S1), S65–S72, DOI: 10.3233/jpd-181476.
12 A. A. Othman, K. Chatamra, M. F. Mohamed, S. Dutta, J. Benesh, M. Yanagawa and M. Nagai, Jejunal infusion of levodopa–carbidopa intestinal gel versus oral administration of levodopa–carbidopa tablets in Japanese subjects with advanced Parkinson's disease, *Clin. Pharmacokinet.*, 2015, **54**(9), 975–984, DOI: 10.1007/s40262-015-0265-3.
13 M. Dangova, N. Ivanova and V. Andonova, Nanocarriers-assisted nose-to-brain delivery of levodopa: current progress and prospects, *Appl. Sci.*, 2025, **15**(1), 331. Available from: https://www.mdpi.com/2076-3417/15/1/331.
14 S. Arisoy, O. Sayiner, T. Comoglu, D. Onal, O. Atalay and B. Pehlivanoglu, In vitro and in vivo evaluation of levodopa-loaded nanoparticles for nose-to-brain delivery, *Pharm. Dev. Technol.*, 2020, **25**(6), 735–747.
15 S. Iravani and R. S. Varma, Plant pollen grains: a move towards green drug and vaccine delivery systems, *Nano-Micro Lett.*, 2021, **13**, 128, DOI: 10.1007/s40820-021-00654-y.
16 M. Lecoeuche, J. Borovička, A. K. F. Dyab and V. N. Paunov, Stimulus-triggered release of actives from composite microcapsules based on sporopollenin from Lycopodium clavatum, *RSC Adv.*, 2024, **14**(15), 10280–10289, DOI: 10.1039/d4ra00236a.
17 C. Yan and S. Kim, Microencapsulation for pharmaceutical applications: a review, *ACS Appl. Bio Mater.*, 2024, **7**(2), 692–710, DOI: 10.1021/acsabm.3c00776.
18 R. C. Mundargi, M. G. Potroz, J. H. Park, J. Seo, E. Tan, J. H. Lee and N. Cho, Eco-friendly streamlined process for sporopollenin exine capsule extraction, *Sci. Rep.*, 2016, **6**, 19960, DOI: 10.1038/srep19960.
19 Y. A. Maruthi and S. Ramakrishna, Sporopollenin – invincible biopolymer for sustainable biomedical applications, *Int. J. Biol. Macromol.*, 2022, **222**, 2957–2965, DOI: 10.1016/j.ijbiomac.2022.10.071.
20 E. Grienenberger and T. D. Quilichini, The toughest material in the plant kingdom: an update on sporopollenin, *Front. Plant Sci.*, 2021, **12**, 703864, DOI: 10.3389/fpls.2021.703864.
21 F. Li, P. Phyo, J. Jacobowitz, M. Hong and J. K. Weng, The molecular structure of plant sporopollenin, *Nat. Plants*, 2019, **5**(1), 41–46, DOI: 10.1038/s41477-018-0330-7.

22 T. Fan, M. G. Potroz, E. Tan, J. H. Park, E. Miyako and N. Cho, Human blood plasma catalyses the degradation of Lycopodium plant sporoderm microcapsules, *Sci. Rep.*, 2019, **9**(1), 2944, DOI: 10.1038/s41598-019-39858-z.

23 V. N. Paunov, G. Mackenzie and S. D. Stoyanov, Sporopollenin micro-reactors for *in situ* preparation, encapsulation and targeted delivery of active components, *J. Mater. Chem.*, 2007, **17**(7), 609–615, DOI: 10.1039/b615865j.

24 A. Diego-Taboada, S. Barrier, M. J. Thomasson and G. Mackenzie, *Pollen: a novel encapsulation vehicle for drug delivery*. 2007. Available from: https://www.researchgate.net/publication/288576554.

25 P. J. Schouten, D. Soto-Aguilar, A. Aldalbahi, T. Ahamad, S. Alzahly and V. Fogliano, Design of sporopollenin-based functional ingredients for gastrointestinal tract targeted delivery, *Curr. Opin. Food Sci.*, 2022, **44**, 100809, DOI: 10.1016/j.cofs.2022.100809.

26 A. Diego-Taboada, L. Maillet, J. H. Banoub, M. Lorch, A. S. Rigby, A. N. Boa, S. L. Atkin and G. Mackenzie, Protein-free microcapsules obtained from plant spores as a model for drug delivery: ibuprofen encapsulation, release and taste masking, *J. Mater. Chem. B*, 2013, **1**(5), 707–713, DOI: 10.1039/c2tb00228k.

27 A. K. F. Dyab, M. A. Mohamed, N. M. Meligi and S. K. Mohamed, Encapsulation of erythromycin and bacitracin antibiotics into natural sporopollenin microcapsules, *RSC Adv.*, 2018, **8**(58), 33432–33444, DOI: 10.1039/c8ra05499a.

28 A. Y. Mohammed, A. K. F. Dyab, F. Taha and A. I. A. El-Mageed, Encapsulation of folic acid into sporopollenin exine capsules: physico-chemical characterisation and controlled release study, *Mater. Sci. Eng., C*, 2021, **128**, 112271. Available from: https://pubmed.ncbi.nlm.nih.gov/34474830/.

29 A. Y. Mohammed, A. K. F. Dyab, F. Taha and A. I. A. El-Mageed, Pollen-derived microcapsules for aspirin microencapsulation: in vitro release and physico-chemical studies, *RSC Adv.*, 2022, **12**(34), 22139–22149, DOI: 10.1039/d2ra02888c.

30 N. M. Meligi, A. K. F. Dyab and V. N. Paunov, Sustained in vitro and in vivo delivery of metformin from plant pollen-derived composite microcapsules, *Pharmaceutics*, 2021, **13**(7), 1048, DOI: 10.3390/pharmaceutics13071048.

31 S. A. Hamad, A. K. F. Dyab, S. D. Stoyanov and V. N. Paunov, Encapsulation of living cells into sporopollenin microcapsules, *J. Mater. Chem.*, 2011, **21**(44), 18018–18025, DOI: 10.1039/c1jm13719k.

32 M. Lorch, M. J. Thomasson, A. Diego-Taboada, S. Barrier, S. L. Atkin, G. Mackenzie and S. J. Archibald, MRI contrast agent delivery using spore capsules: controlled release in blood plasma, *Chem. Commun.*, 2009, **42**, 6442–6444, DOI: 10.1039/b909551a.

33 S. A. Hamad, Self-regulating naturally occurring microcapsules for controlled release of levodopa, *J. Zankoy Sulaimani*, 2019, **21**(2), 81–92, DOI: 10.17656/jzs.10759.

34 Y. Arav and A. Zohar, Model-based optimisation of controlled release formulation of levodopa for Parkinson's disease, *Sci. Rep.*, 2023, **13**(1), 15869, DOI: 10.1038/s41598-023-42878-5.

35 S. Arisoy, Ö. Sayiner and T. Çomoğlu, Development and validation of an in vitro dissolution method for L-Dopa release from PLGA nanoparticles, *Bezmialem Sci.*, 2021, **9**(1), 9–19, DOI: 10.14235/bas.galenos.2020.3860.

36 A. Di Crescenzo, I. Cacciatore, M. Petrini, M. D'Alessandro, N. Petragnani, P. Del Boccio, *et al.*, Gold nanoparticles as scaffolds for antiparkinson codrugs, *Nanotechnology*, 2016, **28**(2), 025102, DOI: 10.1088/1361-6528/28/2/025102.

37 V. Morales, J. McConnell, M. Pérez-Garnes, N. Almendro, R. Sanz and R. A. García-Muñoz, L-Dopa release from mesoporous silica nanoparticles engineered through drug-structure-directing agents, *J. Mater. Chem. B*, 2021, **9**(20), 4178–4189, DOI: 10.1039/d1tb00481f.

38 D. Pentak, V. Kozik, A. Zieba, M. Paździor-Heiske, A. Szymczyk, J. Jampilek and A. Bak, Preparing a liposome-aided drug delivery system: entrapment and release profiles with human serum albumin, *Pharmaceutics*, 2025, **17**(2), 202, DOI: 10.3390/pharmaceutics17020202.

39 L. Illum, Nasal drug delivery—possibilities, problems and solutions, *J. Controlled Release*, 2003, **87**(1–3), 187–198, DOI: 10.1016/s0168-3659(02)00363-2.

40 A. Pires, A. Fortuna, G. Alves and A. Falcão, Intranasal drug delivery: how, why and what for?, *J. Pharm. Pharm. Sci.*, 2009, **12**(3), 288–311, DOI: 10.18433/j3nc79.

41 S. Haque, S. Md, J. K. Sahni, J. Ali and S. Baboota, Development and evaluation of brain-targeted intranasal alginate nanoparticles for treatment of depression, *J. Psychiatr. Res.*, 2014, **48**(1), 1–12, DOI: 10.1016/j.jpsychires.2013.10.011.